A Generative Model of Urban Activities from Cellular Data

Mogeng Yin
Madeleine Sheehan
Sidney Feygin
Jean-Francois Paiement
Alexei Pozdnoukhov
Alexandre Bayen

Electrical Engineering and Computer Sciences
University of California at Berkeley

Technical Report No. UCB/EECS-2017-201
http://www2.eecs.berkeley.edu/Pubs/TechRpts/2017/EECS-2017-201.html

December 12, 2017

Acknowledgement

I would like to thank my advisor in the EECS department Alexandre Bayen for his caring, support and advice in my research and life. I would like to thank my advisor in my home department Alexei Pozdnoukhov for his support and sponsorship, without whom I stand no chance studying in the EECS department and work on such an interesting research problem. I would also like to thank my advisor at AT&T labs research Jean-Francois Paiement for his support and priceless guidance on my research. I would like to thank Professor Randy Katz for reviewing and providing valuable comments on the report.

A Generative Model of Urban Activities from Cellular Data

by

Mogeng Yin

A dissertation submitted in partial satisfaction of the
requirements for the degree of
Master of Science

in

Electrical Engineering and Computer Sciences

in the

Graduate Division

of the

University of California, Berkeley

Committee in charge:

Professor Alexandre M. Bayen, Chair

Fall 2017

A Generative Model of Urban Activities from Cellular Data

Abstract

A Generative Model of Urban Activities from Cellular Data

by

Mogeng Yin

Master of Science in Electrical Engineering and Computer Sciences

University of California, Berkeley

Professor Alexandre M. Bayen, Chair

Activity based travel demand models are becoming essential tools used in transportation planning and regional development scenario evaluation. They describe travel itineraries of individual travelers, namely what activities they are participating in, when they perform these activities, and how they choose to travel to the activity locales. However, data collection for activity based models is performed through travel surveys that are infrequent, expensive, and reflect the changes in transportation with significant delays. Thanks to the ubiquitous cell phone data, we see an opportunity to substantially complement these surveys with data extracted from network carrier mobile phone usage logs, such as call detail records (CDRs). In this paper, we develop Input-Output Hidden Markov Models (IO-HMMs) to infer travelers' activity patterns from CDRs. We apply the model to the data collected by a major network carrier serving millions of users in the San Francisco Bay Area. Our approach delivers an end-to-end actionable solution to the practitioners in the form of a modular and interpretable activity-based travel demand model. It is experimentally validated with three independent data sources: aggregated statistics from travel surveys, a set of collected ground truth activities, and the results of a traffic micro-simulation informed with the travel plans synthesized from the developed generative model.

Contents

List of Figures

List of Tables

Acknowledgments

I would like to thank my advisor in the EECS department Alexandre Bayen for his caring, support and advice in my research and life. I would like to thank my advisor in my home department Alexei Pozdnoukhov for his support and sponsorship, without whom I stand no chance studying in the EECS department and work on such an interesting research problem. I would also like to thank my advisor at AT&T labs research Jean-Francois Paiement for his support and priceless guidance on my research.

Chapter 1

Introduction

Novel mobility paradigms change the transportation landscape quicker than traditional data sources, such as travel surveys, are able to reflect. A vital example is on-demand transportation enabled by a range of services connecting drivers with potential passengers. This increased flexibility of travel options manifests itself in the way citizens structure their day, and causes significant shifts in urban mobility patterns. Public agencies charged with a mandate to manage critical transportation infrastructures are slow to react to these changes, as they are reliant on out-dated information, tools, and models. Part of the problem is the reliance of their methodologies on manually conducted travel surveys.

The National Household Travel Survey (NHTS), the data source that is typically the crux of travel demand models, is conducted every 5 years, and carries a total cost of millions of dollars [18]. NHTS is further limiting because a typical survey only covers two percent of households in a metropolitan area, and typically only records one day of travel per household [32].

At the same time, people generate data while traveling by carrying and using a mobile phone. A valuable alternative is to use a non-invasive, automated, continuous data collection mechanism to complement, supplement, and augment manual surveying. The main advantages are 3-fold: (1) it vastly increases sample size; (2) it eliminates the delays normally associated with administering and processing travel surveys; and (3) it improves activity-based travel modeling by taking advantage of spatially and temporally rich cell phone traces, which capture users activities over months, rather than a single day. While studies of mobility from crowd-sourced locational data are common (these are thoroughly reviewed in Section 2), no existing work provides models in the form that transportation practitioners actually require.

Typical activity-based travel models used by practitioners are incredibly rich in describing the intricacies of human activities and context of decision making in travel-related choices. For years, discrete choice models of travel included trip purpose as context [4]. It is a significant factor influencing decisions on mode and other attributes of travel. One key research challenge therefore lies in detecting trip purposes ("home", "work", "dining", "shopping", "recreation", etc.) from noisy locational data, such as anonymized mobile phone traces regis-

tered via cellular network, with a level of activity-chain detail that is comparable in richness to that of a specifically designed travel survey.

In this thesis, we develop an approach to annotate user activities that reveal temporal activity profiles and the pattern of transitions between activities. To validate the activity recognition results, we compare the annotated activities with a set of collected ground truth activities, and with aggregated statistics from a conventional travel survey. To validate the model and to show its capability of generating realistic activity chains, we use the model to generate synthetic travel plans of individuals with home and work locations sampled from census data. We show that the generated activity chains are realistic and are consistent with the distribution reported in the travel surveys. The synthetic travel plans are used as inputs to an agent-based microscopic traffic simulator. We validate the resulting traffic volumes against an independent dataset of traffic counts collected on all the major freeways within the region of study.

The contributions of this thesis lie in four aspects:

- We implement an end-to-end processing and inference pipeline from the raw cellular data to the travel demand model and traffic simulation tool that transportation practitioners require.

- To the best of our knowledge, this is the first work using context dependent non-homogeneous generative models of the Input-Output Hidden Markov Model (IO-HMM) architecture to analyze activity patterns from cellular data. We empirically show that our generative model outperforms baseline approaches which ignore contextual information in modeling activity profiles and transitions.

- We test our methodology using a real cellular dataset. We annotate secondary activities such as "recreation", "food", "stop in transit" with strong spatial-temporal evidence. We also estimate heterogeneous context-dependent transition probabilities. To validate the model, we compare our annotations to "ground-truth" land-use information of buildings with short range distributed antenna systems, compare the learned activity patterns with travel survey results, and finally compare ground truth traffic counts in the San Francisco Bay Area to a micro-simulation of travel plans derived from the generative model.

- A distributed implementation of the learning and inference methods in a MapReduce framework in pySpark is available at `https://github.com/Mogeng/IO-HMM`. It includes IO-HMM extended with multiple output models such as multinomial logistic regression, generalized linear models, and neural networks.

Chapter 2

Related Work

Urban computing, as an interdisciplinary field, has drawn increasing attention in the recent decade [38]. Urban activity recognition, as a subject of urban computing, has been explored extensively by researchers in different areas. A summary of relevant developments in urban activity modeling is given below with respect to the main data types and the properties of the explored algorithms.

2.1 Locational Data Sources

GPS

GPS data is granular in both spatial and temporal resolution. GPS records sometimes come with additional accelerometer data, but are usually available for a very limited sample of the population. It gave rise to early work in building discriminative state-space models to extract places and activities. Some successful methods unified the process of map matching, place detection, and significant activity inference through a hierarchical conditional random field (CRF) [27].

CDR

The anonymized Call Detail Records (CDRs) from cellular network operators provide a compromise between spatial-temporal resolution and ubiquity. Due to its relatively poor resolution in space, CDR data has been mainly used to derive spatially aggregated results such as mass movements of population [8], aggregated origin-destination (OD) estimation [34], stylized mobility laws [16, 33], and disaster response [29]. Not much work has been done in the area of urban activity recognition, especially for secondary activities. Farrahi, et al., applied Latent Dirichlet Allocation (LDA) and Author Topic Models (ATM) to cluster daily CDR trajectories [13]. However, their model only considered the temporal aspect of CDR data and can only discover activities related to home and work. Phithakkitnukoon, et al., used auxiliary land use data and geographical information database to mine possible

activities around a certain cell tower [30]. However, their model only considers the spatial aspect of CDR data and their assignment of activities is deterministic. The study of most direct relevance to our work is by [35]. It used similar temporal-spatial features to infer urban activities with an undirected relational Markov network. However, one major drawback of their model is the lack of cliques for consecutive activities, i.e., the study did not model activity transitions. This is unfavorable for activity inference and new sample generation. Sampling consecutive activities independently without considering the dependencies of following activities to previous activities is only partly appropriate. To overcome this drawback, we explicitly model contextual dependent activity transition probabilities to improve the accuracy of activity inference and the reliability of new activity chain generation, as detailed in Section 4.1. Validations of models using CDR data are usually difficult due to its low spatial resolution. In addition to the validation through comparing aggregated statistics with travel survey by [35], we provide a direct validation on activity recognition using a set of "ground truth" activities based on short range antennas. We also validated our model with an end-to-end demonstration from raw CDR to the resulting traffic flow volumes produced by a microscopic traffic simulation.

LBSN

Locational-based social network (LBSN) data is usually exact in locations, and may provide additional social relation, comments and reviews of the locations. However it is further limited by the discontinuity between subsequent check-ins. Moreover, users rarely check-in at home and work, which are crucial locations needed for accurate mobility models. Cho, et al., developed a period and social mobility model (PSMM) to separate social trips from commute trips [7]. Ye, et al., created an extended HMM model that incorporated spatial and temporal covariates to classify activities into one of 9 distinct categories [36]. Kling applied a probabilistic topic model to obtain a decomposition of the stream of digital traces into a set of urban topics related to various activities [23].

2.2 Methods and Approaches

Supervised models

Supervised learning methods require data with labeled ground truth. The ground truth is either manually labeled [10, 15], or collected for a small group of participants from a survey accompanying GPS data [22]. Liu, et al., classified activities into "home", "work/school", "non-work obligatory", "social visit" and "leisure" using different supervised learning models including SVM and decision trees. Their data was collected from natural mobile phone communication patterns of 80 users over a year with labeled ground truth [28]. Liao, et al., manually labeled ground truth to extract places and activities [26, 27]. However, this model was only applied to 4 people and is not scalable to large populations.

Unsupervised models

On the other hand, unsupervised models are used to cluster activities with similar temporal and spatial profiles. "Eigenbehavior" models by Eagle et al. [9] and previously mentioned LDA and ATM models by [13, 12] all fall into this category.

Discriminative models

Discriminative state-space models such as CRFs [26, 27] are more flexible when modeling the relationship between input, output and state variables. However, due to their undirected nature, discriminative state-space models cannot be used for activity generation directly.

Generative models

Hidden (semi-) Markov models are generative models that can not only be used to analyze activity patterns, but also to generate new sequences [17]. Using GPS data, Baratchi, et al., developed a hierarchical hidden semi-Markov-based model that captures both frequent and rare mobility patterns in the movement of mobile objects [3].

Chapter 3

Modeling Framework

In this work, not only are we interested in understanding the activity patterns themselves. We also aim to model these patterns in a generative probabilistic framework suitable for generating inputs to activity based travel micro-simulations. Thus, we require generative models. At the same time, privacy considerations and limited availability of ground truth location data preclude us from using discriminative supervised approaches, suggesting the choice of unsupervised models. In order to produce activity patterns for large populations of users, we build models that can leverage distributed implementation and that can share parameters across multiple user groups. These objectives led us to an IO-HMM approach with modular heterogeneous transitions/emissions components with interpretable parameters, as detailed in Section 4.

The developed data processing and modeling pipeline is presented in Fig. 3.1. The left column shows the primary data sources. This includes the cellular call detail data (CDR), a comprehensive point of interest (POI) database within the region of interest, and the traffic data (vehicle counts, volumes) to calibrate and validate the microscopic traffic simulation. POI databases are usually available from open source maps such as OpenStreetMap, or comercial APIs such as Google Places API and Factual Places API. These POI databases provide a list of POIs and their category labels around a location upon query. These POI information is useful in constructing the labeled activities as "ground truth". The middle column contains the key modules to perform inference and the right column shows the resulting products. Our key contribution is the Activity Recognition and Generation module outlined with the red dashed rectangle, and in particular the components shown in shaded yellow.

Raw CDR data contains a timestamped record for each communication of anonymous user's devices served by the cellular network. Due to positioning errors and connection oscillations, it is not straightforward to extract features to perform activity recognition from raw CDR sequences. A pre-processing step is first performed to convert the records to a sequence of stay location clusters that may correspond to distinct yet unlabeled activities, as shown in Fig. 3.2. The clustering can be seen as a first layer of hashing locations, which preserves privacy. Attributes of each activity, such as the start time, duration, location fea-

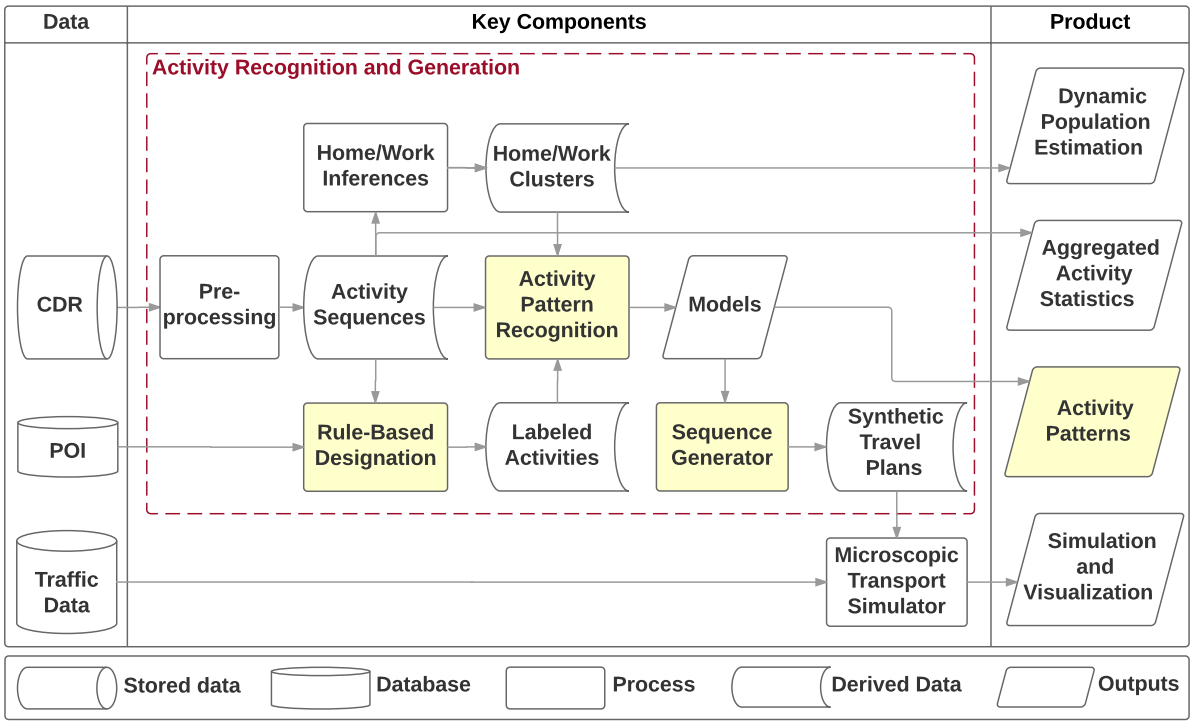

Figure 3.1: Modeling framework diagram. The left column represents the input to the research; the middle column represents the key modeling components; and the right column represents the products of the research. Our key contribution of activity recognition and generation module are outlined with the red dashed rectangle, and the key components are shown in shaded yellow.

tures, and the context of the activity (whether this activity happens during a home-based trip, work-based trip, or a commute trip), is also extracted as a result of this processing. The details of this step are presented in Appendix A. From the activity sequences, primary activities such as home and work can be inferred[1], as described in more details in Appendix B. Detecting home and work location features are useful in many respects: first, this allows us to perform dynamic population estimation, as the first product of the pipeline in Fig. 3.1. Second, with home and work inferred, we can identify specific groups of users by a set of predefined decision rules. One of the most simple rules is to group users by their geographical area. This makes it possible to train separate models for users residing in a specific neighborhood or a Transportation Analysis Zone (TAZ) since people living in different geographical zones might show different travel behaviors. Moreover, we can train separate models for regular commuters/part-time/unemployed groups of residents within a community. The model structures are expected to be significantly different within each

[1]Note that once the pre-processing and home/work inference steps are applied, only features associated with location clusters are used for modeling, such as distances to home and work. This can be seen as a second layer of anonymization of user's locations, since no specific location cluster IDs are associated with any user at any time in the modeling process itself.

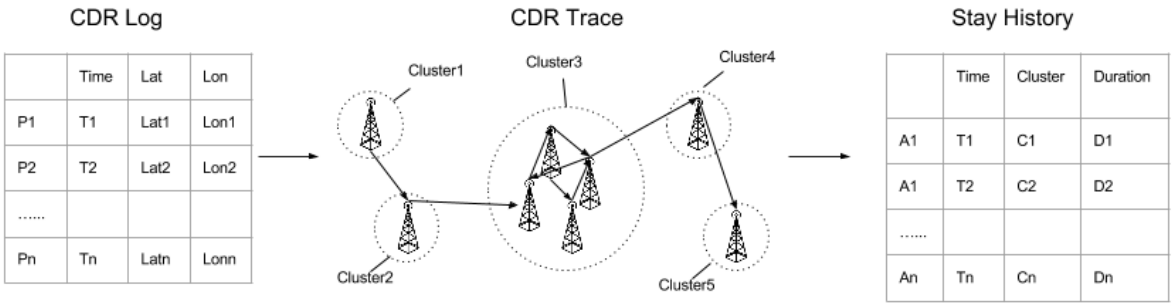

Figure 3.2: Call Detail Records (CDR) data processing. The table at left represents the raw CDR format, i.e., time stamped record of communications. A stay points detection algorithm (detailed in Appendix A) is used to convert the raw CDR data to a sequence of stay locations with start time, duration and location ID, as represented in the table at right.

group. Finally, home and work inference for anonymized cellular users adjusted to the full population provides daytime/nighttime population density estimates, as shown in Fig. 5.2.

With the activity sequences (including home and work anchor activities) identified, we can understand the daily activity structure of travelers that are traditionally available solely via manual surveying. They include: (1) the distribution of number of tours before going to work, during work and after getting back home; (2) the distribution of number of stops during each type of tour (home-based, work-based and commute tours); and (3) the interactions in stop-making across different times of day (e.g. how making an evening commute stop will affect the decision in making a post-home stop) [6]. This is the second product of this research as listed in Fig. 3.1. With the processed activity sequences and inferred primary activities, we can perform the secondary activity recognition and analyze the activity patterns, including spatial-temporal profiles of activities and activity transition probabilities. The resulting models and analysis will be the third product of the research. To validate the recognition results, we collected a small set of ground truth activities based on short range antennas which have relatively high spatial resolution. Point of interests (POI) data are joined with these short range antennas to identify the possible activities performed there and a set of rules are used to help us collect labeled activities, as detailed in Section 4.3. With the model coefficients and a set of sampled home and work locations of the total population, we can generate activity sequences and produce synthetic travel plans required by a microscopic traffic simulator. Ground truth traffic counts data are used to validate the simulation results and showcase the validity of the presented work for transportation planning and operations practice. This is the fourth product in Fig. 3.1.

Chapter 4

Activity Recognition and Generation

This section introduces main modeling components shown within the red dashed box in Fig. 3.1, including activity pattern recognition with IO-HMM, a method of collecting ground truth activities from short range distributed antenna systems, and a method of simulating activity chains from the resulting models.

4.1 IO-HMM for Activity Pattern Recognition

Given the user stay history, that is, a list of stay location features with start times and durations, we would like to convert it into a sequence of activities enriched with semantic labels ("shopping", "leisure", etc.), and a heterogeneous context-dependent probability model of transitions between the activities.

IO-HMM Architecture

Hidden Markov Models (HMMs) have been extensively used in the context of action recognition and signal processing. However, standard HMMs assume homogeneous transition and emission probabilities. This assumption is overly restrictive. For instance, if a user engages in a home activity on a weekday, and departs for the next activity in the morning, she is likely going to work. If she departs in the evening, the trip purpose is likely to be recreation or shopping. Therefore, we propose to use the IO-HMM architecture that incorporates contextual information to overcome the drawbacks of the standard HMM. In Fig. 4.1, the solid (blue) nodes represent observed information, while the transparent (white) nodes represent latent random variables. The top layer contains the *observed* contextual variables $\boldsymbol{u_t}$, such as time of day, day of the week, and information about activities in the past (such as the number of hours worked on that day). Note that the values of the input variables $\boldsymbol{u_t}$ used to represent the context have to be known prior to a transition. The middle layer contains *latent* categorical variables z_t corresponding to unobserved activity types. The bottom layer

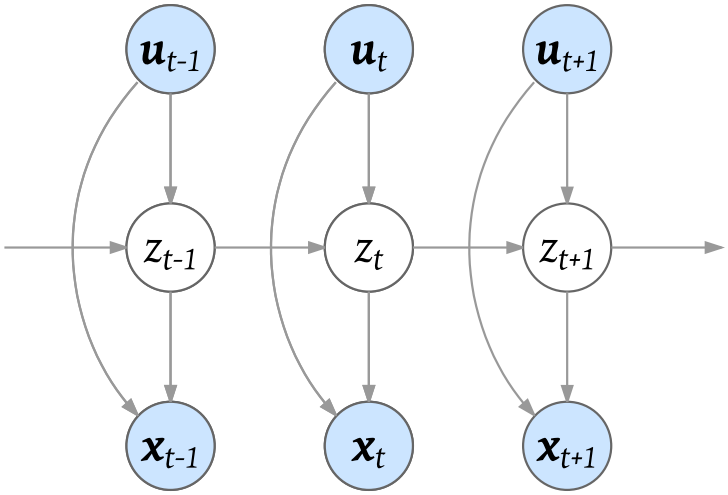

Figure 4.1: IO-HMM Architecture. The solid nodes represent observed information, while the transparent (white) nodes represent latent random variables. The top layer contains the *observed* input variables $\boldsymbol{u_t}$; the middle layer contains *latent* categorical variables z_t; and the bottom layer contains observed output variables $\boldsymbol{x_t}$.

contains observed variables $\boldsymbol{x_t}$ that are available during training of the models (but not when generating activity sequences), such as location features and duration of the stay.

Likelihood of a data sequence under this model is given by:

$$\begin{aligned} L(\boldsymbol{\theta}, \boldsymbol{x}, \boldsymbol{u}) \;=\; & \sum_{\boldsymbol{z}} \Big(\Pr(z_1 \mid \boldsymbol{u_1}; \boldsymbol{\theta_{in}}) \cdot \\ & \prod_{t=2}^{T} \Pr(z_t \mid z_{t-1}, \boldsymbol{u_t}; \boldsymbol{\theta_{tr}}) \cdot \\ & \prod_{t=1}^{T} \Pr(\boldsymbol{x_t} \mid z_t, \boldsymbol{u_t}; \boldsymbol{\theta_{em}}) \Big). \end{aligned} \tag{4.1}$$

IO-HMM architecture has been well described in [5]. Variable notation and important differences between IO-HMM and standard HMM are summarized in Table 4.1.

Parameter Estimation

IO-HMM includes three groups of unknown parameters: initial probability parameters ($\boldsymbol{\theta_{in}}$), transition model parameters ($\boldsymbol{\theta_{tr}}$), and emission model parameters ($\boldsymbol{\theta_{em}}$). Expectation-Maximization (EM) is a widely used approach to estimate the parameters of IO-HMM. The EM algorithm consists of two steps.

E step: Compute the expected value of the complete data-log likelihood, given the observed data and parameters estimated at the previous step.

Table 4.1: Highlights of comparison between an HMM versus. IO-HMM ($\boldsymbol{u_t}$, z_t, $\boldsymbol{x_t}$ denote input, hidden and output variables respectively, i is an index of a hidden state, t is a sequence timestamp index).

	HMM	IO-HMM
initial state probability π_i	$\Pr(z_1 = i)$	$\Pr(z_1 = i \mid \boldsymbol{u_1})$
transition probability $\varphi_{ij,t}$	$\Pr(z_t = j \mid z_{t-1} = i)$	$\Pr(z_t = j \mid z_{t-1} = i, \boldsymbol{u_t})$
emission probability $\delta_{i,t}$	$\Pr(\boldsymbol{x_t} \mid z_t = i)$	$\Pr(\boldsymbol{x_t} \mid z_t = i, \boldsymbol{u_t})$
forward variable $\alpha_{i,t}$	$\delta_{i,t} \sum_l \varphi_{li,t} \alpha_{l,t-1}$, with $\alpha_{i,1} = \pi_i \delta_{i,1}$	
backward variable $\beta_{i,t}$	$\sum_l \varphi_{il,t} \beta_{l,t+1} \delta_{l,t+1}$, with $\beta_{i,T} = 1$	
complete data likelihood L_c	$\sum_i \alpha_{i,T}$	
posterior transition probability $\xi_{ij,t}$	$\varphi_{ij,t} \alpha_{i,t_1} \beta_{j,t} \delta_{j,t} \,/\, L_c$	
posterior state probability $\gamma_{i,t}$	$\alpha_{i,t} \beta_{i,t} \,/\, L_c$	

M step: Update the parameters to maximize the *expected* data likelihood given by:

$$
\begin{aligned}
Q\left(\boldsymbol{\theta}, \boldsymbol{\theta^k}\right) &= \sum_{i=1} \gamma_{i,1} \log \Pr\left(z_1 = i \mid \boldsymbol{u_1}; \boldsymbol{\theta_{in}}\right) \\
&+ \sum_{t=2}^{T} \sum_i \sum_j \xi_{ij,t} \log \Pr\left(z_t = j \mid z_{t-1} = i, \boldsymbol{u_t}; \boldsymbol{\theta_{tr}}\right) \\
&+ \sum_{t=1}^{T} \sum_i \gamma_{i,t} \log \Pr\left(\boldsymbol{x_t} \mid z_t = i, \boldsymbol{u_t}; \boldsymbol{\theta_{em}}\right). \qquad (4.2)
\end{aligned}
$$

In the above, $Q\left(\boldsymbol{\theta}, \boldsymbol{\theta^k}\right)$ is the expected value of the complete data log likelihood; k represents the EM iteration; T is the total number of timestamps in each sequence; $\boldsymbol{u_t}$, z_t and $\boldsymbol{x_t}$ are the inputs, hidden states, and observations at step t; and $\boldsymbol{\theta}$ are the model parameters to be estimated. The meaning of other variables is given in the first column of Table 4.1.

Transition and Emission models

The parameter estimation procedure of IO-HMM described above implies that any supervised learning model that supports gradient ascent on the log probability can be integrated into the IO-HMM. For example, in Equation 4.2, each of the model parameters ($\boldsymbol{\theta}$) can be estimated with neural networks. A neural network with a softmax layer can be used to learn the initial probability parameters ($\boldsymbol{\theta_{in}}$) through back-propagation, another neural network with a softmax layer for learning the transition probability parameters ($\boldsymbol{\theta_{tr}}$), and a third with customized layers for estimating emission model parameters ($\boldsymbol{\theta_{em}}$).

Note that the EM algorithm can be naturally implemented in a MapReduce framework, a programming model and an associated implementation for processing large data sets on

computing clusters. The Expectation step can be fit into the Map step, calculating the posterior state probability γ and posterior transition probability ξ in parallel for each training sequence. The estimated posterior probabilities γ and ξ are collected in the Reduce step. The source code of an implementation developed as a part of this research is available from `https://github.com/Mogeng/IO-HMM`.

4.2 Model Specification

Input-Output Variables

In practice, models of simple structure (linear, multinomial logistic, Gaussian) with interpretable variables and parameters are preferred. For example, in an application below, we include the following input variables $\boldsymbol{u_t}$: (1) a binary variable indicating whether the day is a weekend; (2) five binary variables indicating the time of day that the activity starts, morning (5 to 10am), lunch (10am to 2pm), afternoon (12 to 2pm), dinner (4 to 8pm) or night (5pm to midnight); and (3) for the users with identified work location, the number of hours the user has spent at work this day. This variable contains accumulated knowledge on the past activities.

The IO-HMM model also includes the following outputs $\boldsymbol{x_t}$ at each timestamp t: (1) $x^{(1)}$, the distance between the current stay location and the user's home; (2) $x^{(2)}$, the distance between the current stay location and the user's work place; (3) $x^{(3)}$, the duration of the activity; and (4) $x^{(4)}$, whether the user has visited this stay location cluster previously.

The selection of the inputs and outputs is guided by common knowledge. The activity start time is relevant for differentiating activity types. The number of hours worked in a day is a strong indicator of a person's likelihood to return to work (after a midday activity, for example). The model inputs contain information that is known at the start of the transition to a new activity. In contrast, the output features contain information that is not available at the transition to a new activity. For example the duration and the location or land-use in the vicinity of a new activity is unknown at the time of the transition. In other words, output variables can be observed when training the models, but must be inferred when sampling sequences of activities from the model.

The model outputs have a strong dependence on the activity type. For example, the distance that a person is willing to travel from home for a leisure trip may be longer than the distance that a person is willing to travel for a shopping trip. The duration depends both on the activity type, activity start time, and on the previous activities in the day. e.g., the expected duration of a work activity will decrease if a person has already worked in the day.

Initial, Transition and Emission Models

Multinomial logistic regression models are used as the initial probability model and transition probability models. Note that for succinctness, we use $\boldsymbol{\theta}$ in each of the following equations to represent the $\boldsymbol{\theta_{in,tr,em}}$ in Equation 4.2. The first term of Equation 4.2 can be written as:

$$\Pr\left(z_1 = i \mid \boldsymbol{u_1}; \boldsymbol{\theta}\right) = \frac{e^{\boldsymbol{\theta^i u_t}}}{\sum_k e^{\boldsymbol{\theta^k u_t}}}. \tag{4.3}$$

The $\boldsymbol{\theta}$ for initial probability model is a matrix with the i^{th} row ($\boldsymbol{\theta^i}$) being the coefficients for the initial state being in state i. The second term of Equation 4.2 can be written as:

$$\Pr\left(z_t = j \mid z_{t-1} = i, ; \boldsymbol{\theta}\right) = \frac{e^{\boldsymbol{\theta_i^j u_t}}}{\sum_k e^{\boldsymbol{\theta_i^k u_t}}}. \tag{4.4}$$

The $\boldsymbol{\theta}$ for transition probability models is a set of matrices with the j^{th} row of the i^{th} matrix ($\boldsymbol{\theta_i^j}$) being the coefficients for the next state being in state j given the current state being in state i.

To gain interpretability, we use linear models for the outputs represented as continuous random variables. We assume a Gaussian distribution for the distance to home and work variables $x^{(1)}$ and $x^{(2)}$ and the activity duration variable $x^{(3)}$. Where $x^{(1)}$ and $x^{(2)}$ depend only on the hidden activity type, the duration variable $x^{(3)}$ depends on the hidden activity and also the contextual input variables. The third term of Equation 4.2 can be written as:

$$\Pr\left(x_t \mid z_t = i, \boldsymbol{u_t}; \boldsymbol{\theta_i}\right) = \frac{1}{\sqrt{2\pi}\sigma_i} e^{-\frac{(x_t - \boldsymbol{\theta_i} \cdot \boldsymbol{u_t})^2}{2\sigma_i^2}}, \tag{4.5}$$

The $\boldsymbol{\theta}$ for one such output emission model is a set of arrays where $\boldsymbol{\theta_i}$ and σ_i denote the coefficients and the standard deviation of the linear model when the hidden state is i. While we chose to represent outputs $x^{(1),(2),(3)}$ as Gaussian random variables, Gamma regression could be applied to duration $x^{(3)}$ to capture the non-negative, continuous, and right-skewed nature of these response variables. Moreover, response variables $x^{(1)}$ and $x^{(2)}$ could be modeled simultaneously using multivariate linear regression to capture the correlations between distance to home and distance to work.

Output $x^{(4)}$ is a binary variable, and we used logistic regression model as the output model. The probability in the third term of Equation 4.2 can be written as:

$$\Pr\left(x_t = 1 \mid z_t = i, \boldsymbol{u_t}; \boldsymbol{\theta_i}\right) = \frac{1}{1 + e^{-\boldsymbol{\theta_i} \cdot \boldsymbol{u_t}}}. \tag{4.6}$$

Finally, we emphasize that an activity label is just a latent categorical variable. A semantic label can be associated to it following an in-depth analysis the we present in Section 5.2 below.

4.3 Model Selection

Model selection for IO-HMM includes the choice of the number of hidden states. One would like to set a high number that encompasses a wide variety of travel purposes, however, data quality and availability limits the number of feasibly identifiable activities. Moreover, an ambiguity in semantic meaning of activity types (consider "leisure" versus "recreation") asks for limiting the number of hidden states that show useful in practical applications. We describe here an empirical procedure for collecting ground truth data on activity types that provide useful insights on these modeling choices. The number of hidden states of the IO-HMM model are set according to the labels of these ground truth activities. For CDR, it is usually hard to collect ground truth activities due to its low spatial resolution. However, there is a set of short range antennas that serve only a small range of area, which have relatively high spatial resolution. These short range antennas provide us the opportunity to collect "ground truth" activities.

Short Range Distributed Antenna Systems (DASs)

A common component of a cellular networks is a set of distributed antenna systems (DASs) that are short ranged, including Indoor DASs (IDASs) and Outdoor DASs (ODASs). IDASs are usually installed in large commercial buildings such as shopping malls to ensure better signal coverage. And ODASs are usually installed at high occupancy outdoor venues such as stadiums or concert arenas. These antennas are set up to maximize signal strength for the users located in the building or stadium served by a given DAS, ensuring more precise localization. Fig. 4.2 illustrates the times and durations of connections established by users served by three particular DASs. The patterns are structured in time, indicating the activities performed there are quite regular and their purpose can be inferred from domain knowledge with high confidence.

Designation of Rules for Ground Truth

IDASs are often installed in large mixed-use commercial buildings. For example, one commercial building with IDAS installed could have bakeries, restaurants, taxi stands, gym and fitness centers, retail stores, as well as other businesses such as accounting and financial services. We designed a set of spatial-temporal decision rules to label a set of activities that can be considered as the ground truth. For instance, if a user is connected to a DAS in a food court at noon for one hour, this is most likely to be indicative of a lunch activity. Although we do not have complete certainty that this is indeed the activity type, the event is indistinguishable from a lunch break in terms of its mobility footprint, and with high likelihood we interpret this as a food activity.

We first acquired place information from POI databases such as Google places API and Factual Global Places API. Then, we joined this information with the locations of the DASs in order to extract activities that could be performed at each DAS. The place information

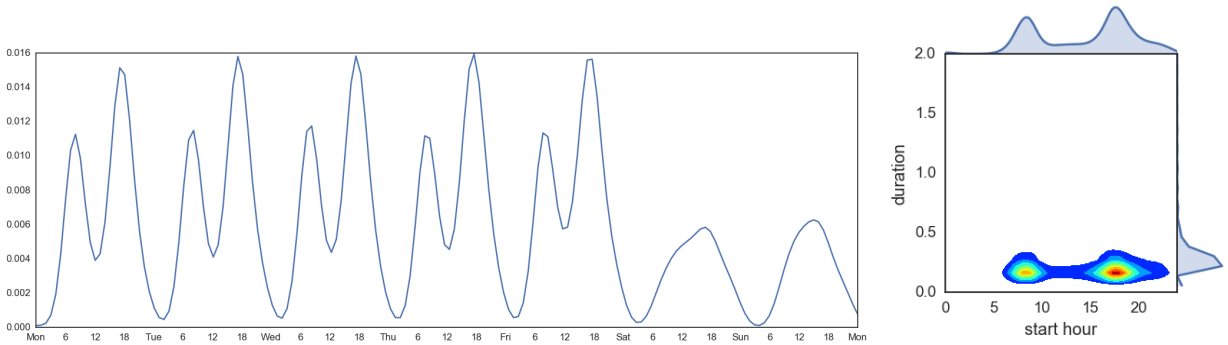

(a) DAS in a major train station used by suburban commuters.

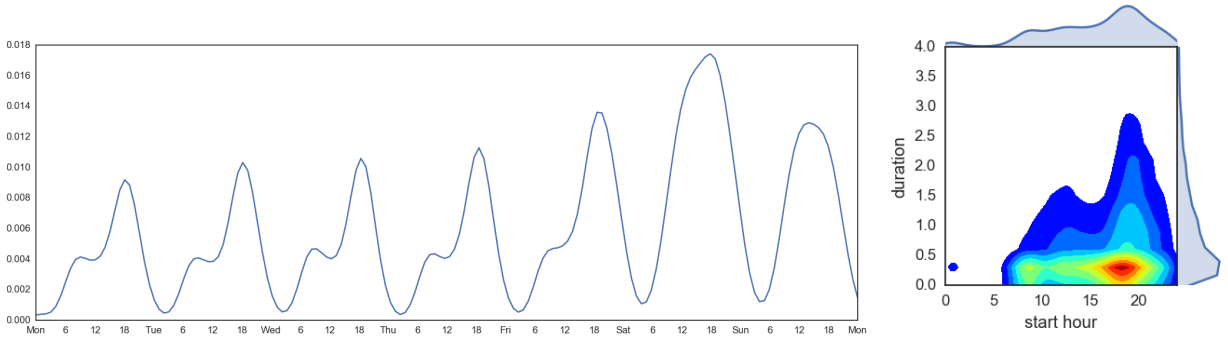

(b) DAS in a fitness center with multiple recreational health studios.

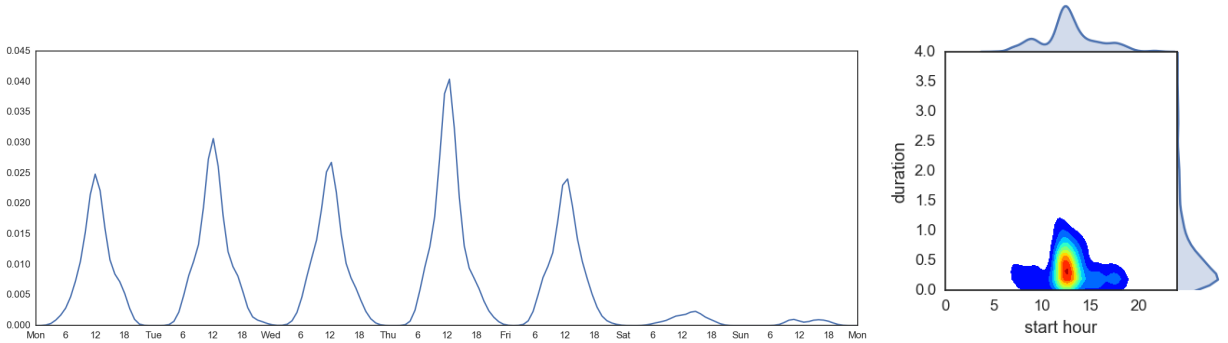

(c) DAS in a business district building with a large food court.

Figure 4.2: Structural patterns of empirical data collected at short range DASs well explain the activity performed around the DASs: the number of activities start times within a course of a week (left) and an empirical joint distribution plot of the visit duration versus start times (right).

Table 4.2: Rules of labeling secondary activities based on activity spatial-temporal features

Activity	Duration (hours)	Start hour	Context	Location category
Lunch	0.25 - 1	11-12		Food
Dinner	0.25 - 2	17-18		Food
Shop	0.25 - 1	7-9 14-15 20-21	Home based or during evening commute	Shop
Transport	< 0.25		Commute	Transport
Recreation	1-4	7-21	Home based or during evening commute	Recreation
Personal	any	7-21		Personal
Travel	any	any		Out of the region

provides listings of local business and point of interest (POI) at most given locations. Since multiple activities can happen at the same location, we need some additional rules based on the spatial-temporal features of activities, as shown in Table 4.2. The "location category" column of the table indicates that the category is among the category labels returned from the APIs.

Note that the rules used to label activities as reported in Table 4.2 are restrictive. Given that the main purpose of these labels is to validate the proposed models, our goal is to be very confident in the activities we label. Thus, these rules are designed to pursue high precision rather than high coverage.

4.4 Activity Chains Generation

One of the strengths of the proposed generative state-space model is that it can generate sequences of activities based on the parameters $\boldsymbol{\theta}$ estimated for each user or shared across a group of users believed to have similar mobility lifestyle. For example, a working day scenario can be generated as follows. A synthetic population with a predetermined home and work locations is created according to the population census. Each user is assumed to begin her day at home, $z_1 = 0$. Relevant context information $\boldsymbol{u_t}$ and learned transition $\Pr(z_t = j \mid z_{t-1} = i, \boldsymbol{u_t})$ and emission probabilities (4.5)-(4.6) are then used to determine the next state and sample output variables for the activity duration and location from the posterior. At the end of this activity the relevant context information $\boldsymbol{u_t}$ is updated and the next activity is selected given the newly obtained transition probabilities. The process continues until the full daily sequence of activities has been generated. We discuss the interpretation of the posterior probability distributions and report on an experimental validation of this approach below.

Chapter 5

Experimental Results

This section describes a full-scale regional experiment where we train IO-HMM for commuters from each of the 34 super-districts in the San Francisco Bay Area, in order to develop an actionable mobility model for a typical weekday. First we show how one can interpret the model parameters and evaluate activity recognition capability, using the City of San Francisco (SF) as an example. Next, we use the trained models for all 34 super-districts to generate sequences of activities for a regional agent-based traffic micro-simulation, and compare the results with the observed traffic volumes.

The data used in these studies comprise a month of anonymized and aggregated CDR logs collected in Summer 2015 by a major mobile carrier in the US, serving millions of customers in the San Francisco Bay Area. No personally identifiable information (PII) was gathered or used for this study. As described previously, CDR raw locations are converted into highly aggregated location features before any actual modeling takes places.

5.1 Data Pre-processing

We pre-process the data following the steps in Appendix A. The home and work locations are identified during the pre-processing step. We take cell phone users that:

- showed up for more than 21 days a month at their identified "home" place;
- showed up for more than 14 days a month at their identified "work" place;
- have home and work **not** at the same location.

These criteria identify regular working commuters with a day structure containing both distinct Home and Work. Empirical distributions of the average number of daily activities for this population is shown in Fig. 5.1. The median number of activities is 4.4 per weekday and 4.0 per weekend. This is consistent with the California Household Travel Survey, reporting a number of 4 activities per day [1].

Fig. 5.2 shows the density map of inferred home and work locations for San Francisco residents, aggregated at the census tract level. As shown in the right of Fig. 5.2, the work

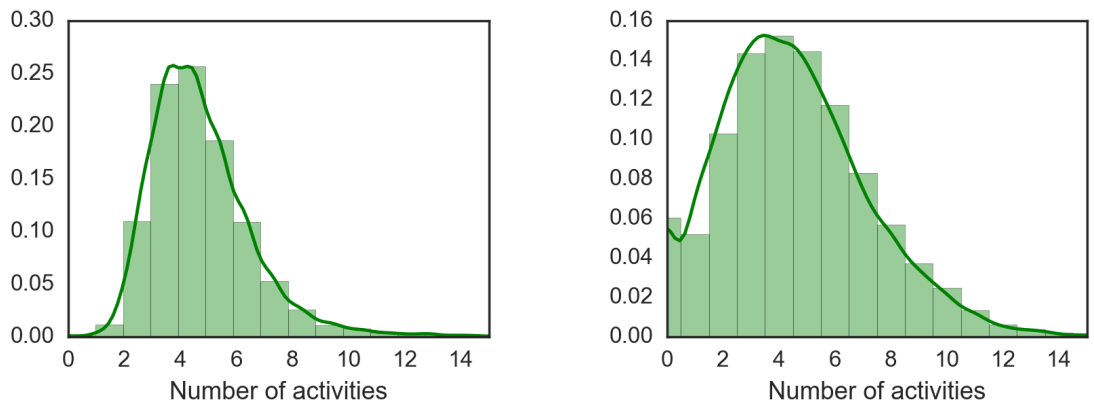

(a) Weekday (b) Weekend

Figure 5.1: Empirical distributions of the average number of daily activities of San Francisco subscribers on a weekday (left) and on a weekend (right), after pre-processing.

locations are spread in the SF Bay Area. The highest density occurs in San Francisco, Oakland, and some South Bay cities. Focusing on work locations in San Francisco, many of the inferred work locations are in Downtown San Francisco, the Financial District, and SoMA - three San Francisco neighborhoods with high employment density [21]. As expected, the home locations are more spread out throughout the city.

While individual users with long sequences of observations can be modeled with fully personalized IO-HMM, such processing violates privacy protection regulations of the carrier. An application of the IO-HMM presented below is trained with parameters shared across a group of users with similar geographical and structural properties of the day. It not only provides computational advantages, but also simplifies scenario evaluation for the practitioners who operate with socio-demographic groups rather than individuals. In this paper, we simplified the grouping method to be based on geographical boundaries, such as super-districts defined by the San Francisco Metropolitan Transportation Commission (MTC).

5.2 Activity Recognition Results

In this section we interpret the results of the IO-HMM that has been fit to the four super-districts that make up the city of San Francisco. The model was trained on a group of 20,000 anonymous San Francisco residents (about 2% of the population). The coefficients of trained emission models are reported in Table 5.1. Recall that we use linear models as the output models for $x^{(1)}$, distance to home, $x^{(2)}$, distance to work, and $x^{(3)}$, duration of the activities. Logistic regression was used as the output model for $x^{(4)}$, cluster has been visited before. Since $x^{(1)}$ and $x^{(2)}$ depend only on the hidden activity, only the intercepts are estimated. For $x^{(3)}$, we specify that the duration depends on activity type and also on the "day of week", "time of day" and "hours worked" input variables, there are 8 coefficients

Figure 5.2: Density map of inferred home and work locations for San Francisco residents, aggregated at the census tract level (left), and an overall geographical scope of analysis with work locations density (right).

Table 5.1: Model coefficients for the output variables per hidden activity (see interpretation in the text).

State: latent activity	Dist to home	Dist to work	Duration								Visited	
			constant	weekend	morning	lunch	afternoon	dinner	evening	hours worked	no	yes
0: Home	0.00	7.22	9.45	2.17	-6.29	-2.57	-0.94	0.20	1.29	-0.03	0	2.19
1: Work	7.22	0.00	4.00	-0.02	2.98	0.76	0.19	-0.64	-0.10	-0.26	0	1.76
2: Food/Shop	2.37	1.90	0.84	0.18	0.00	-0.01	-0.04	-0.01	0.25	0.00	0	-0.53
3: Stop in Transit	3.21	3.63	0.16	0.00	-0.01	0.00	0.00	0.00	0.00	0.00	0	-0.46
4: Recreation	2.36	15.03	2.76	0.17	-0.42	-0.64	-0.45	-0.68	0.37	0.04	0	-0.44
5: Personal	18.79	16.94	0.93	0.46	0.17	0.12	-0.05	-0.03	-0.05	0.01	0	-1.35
6: Distant Travel	787.94	784.71	4.26	0.78	-0.75	-0.39	-0.76	-1.27	1.11	0.29	0	-1.17

estimated per hidden state for this output. Since $x^{(4)}$ "has visited" is a binary variable, only one parameter per hidden state is identifiable.

Two temporal representations help identify the latent semantics of the hidden states (i.e. activities). Fig. 5.3 depicts the distribution of start times of activities. The y-axis gives the number of activities started at a given hour. By evaluating these weekly activity start-time patterns in combination with the output coefficients in Table 5.1, and the joint distribution of start time and duration in Fig. 5.4 we can assign semantic labels for activity type to each of latent activity states.

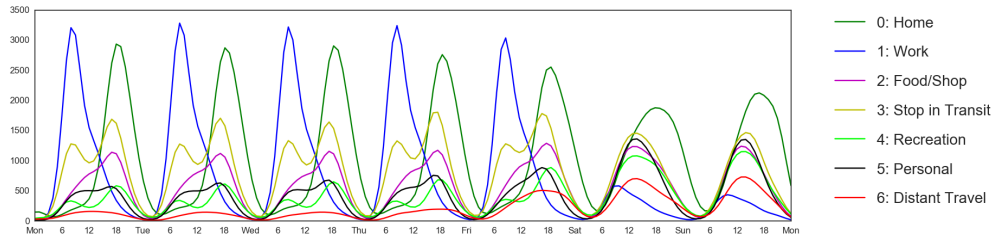

Figure 5.3: Number of activities (labeled per highest posterior probability) by their respective start time within a course of a week.

Primary Activities: Home and Work

Latent activity state 0, shown in green in Fig. 5.3 is easily identifiable - it is the "home" activity. The typical start time ranges from 3pm to midnight. The home activity exhibits greater variation in start time on Friday and weekends than on other weekdays. The positive "weekend" coefficient on the duration of this activity indicates that people stay at home longer during weekends.

The temporal profile of home activities in Fig. 5.4a has two major clusters. The upper cluster indicates regular overnight home activities. This cluster can be further separated into two clusters. One peaks at 6pm, representing the home activity directly after work. The other peaks at 9pm, representing the home activity after some secondary activities in the evening. Since the home activity duration is generally set by the regular work start hour, the downward slope of the upper cluster signifies that if a user arrives at home later in the day, they are likely to spend fewer hours at home.

Activity state 1, shown in blue in Fig. 5.3 is the "work" activity. It has highest peaks in Fig. 5.3, signifying that it is a very regular activity with concentrated start times.

According to Table 5.1, a work activity has a base duration of 4 hours, if it starts in the morning, the user is likely to stay 2.98 hours longer, that is 6.98 hours in total; if it begins in the afternoon or evening the average duration is shorter. As a compounding effect of returning to work in the afternoon or evening, the "hours worked" column indicates that the expected duration will decrease by 0.26 hours for every hour that the user already spent at work in the day. The "is weekend" column indicates that if a user chose to work on weekend, the average work activity duration is not significantly different from that on weekdays; note that (from Fig. 5.3) the probability of visiting the work activity is much lower on the weekend. The "visited" column indicates the propensity of the location being frequently revisited. For the work activity, the coefficient 1.76 indicates a very high likelihood of returning to the same location to perform the same activity.

From Fig. 5.4b, we can see that the temporal profile of work activities has three clusters. The upper cluster indicates regular "9 to 5" work activities without a break. The lower left cluster represents the morning work activities and the lower right cluster represents the afternoon work activities. All three clusters are tilted at -45 degrees. This is due to the usually fixed lunch hour at noon and end of work at about 5pm.

Secondary Activities

The remaining states are secondary activities. Activity 2 peaks in start time around noon and in the evening. As shown in Table 5.1, activity state 2 has an average duration of about 0.84 hours, and is close to both home and work place. As shown in Fig. 5.4c, the duration of this activity is slightly longer in the evening. Based on these properties, we assign activity 2 the label "food/shop". From Fig. 5.3 we see that, on weekends, this activity peaks at noon. The weekend activity duration, according to Table 5.1, is about 0.2 hours longer than it is on weekdays.

Activity 3 is located close to home and work, and has an average duration of about 10 minutes, according to Table 5.1. From Fig. 5.4e, we can see that this activity peaks in the early morning and late afternoon right before home activity. Fig. 5.4d and Table 5.1 also indicate that the duration is not affected by time of day or day type (weekend versus weekday). From Fig. 5.3, we can see that this activity is visited more frequently on weekdays than weekends, indicating that the activity could be an in-commute activity such as coffee, transport, or picking up kids. It is worth noting that although activity 3 is less revisited than home and work activities, it is more likely to be revisited compared to other activities. This gives us more confidence in labeling them as regular activities such as "Short Stop in Transit".

We have assigned activity state 4 a label of "recreation". As seen in Table 5.1, the activity is quite close to home but far from the work place. The state has an average duration of 2.7 hours, much longer than the durations of activity state 2 and 3. This activity last longer in evening hours or weekends. As shown in Fig. 5.3, this activity often starts in the early morning or evening hours on weekdays, and tellingly, more users engage in this activity on Fridays and weekends.

We have assigned activity state 5 a label of "personal". The distances from home and work are 19 and 17 miles, respectively, and the average duration of this activity is 0.93 hours. This state could encompass both off-site work related trips and/or longer-distance dining or leisure activities. As shown in Fig. 5.3. Due to the distance of this activity, more users engage in this activity on weekends and this activity is least likely to be revisited.

Activity state 6, labeled "distant travel", or more accurately activities that occur while traveling, is the most irregular and infrequent. The average distances from home and work are quite high (average 800 miles). This activity type seems to occur predominantly on Fridays and weekends according to Fig. 5.3.

Activity Transitions

We omitted "distant travel" activity from the transition matrix since if a person is traveling a long distance, the next activity is also most likely to be categorized as "distant travel"; the distance dominates the state. Fig. 5.5a shows the transition matrix associated with mornings. The labels on the left indicate the state the user is transitioning from, and the labels on the top indicate the state the user is transitioning to. The most significant

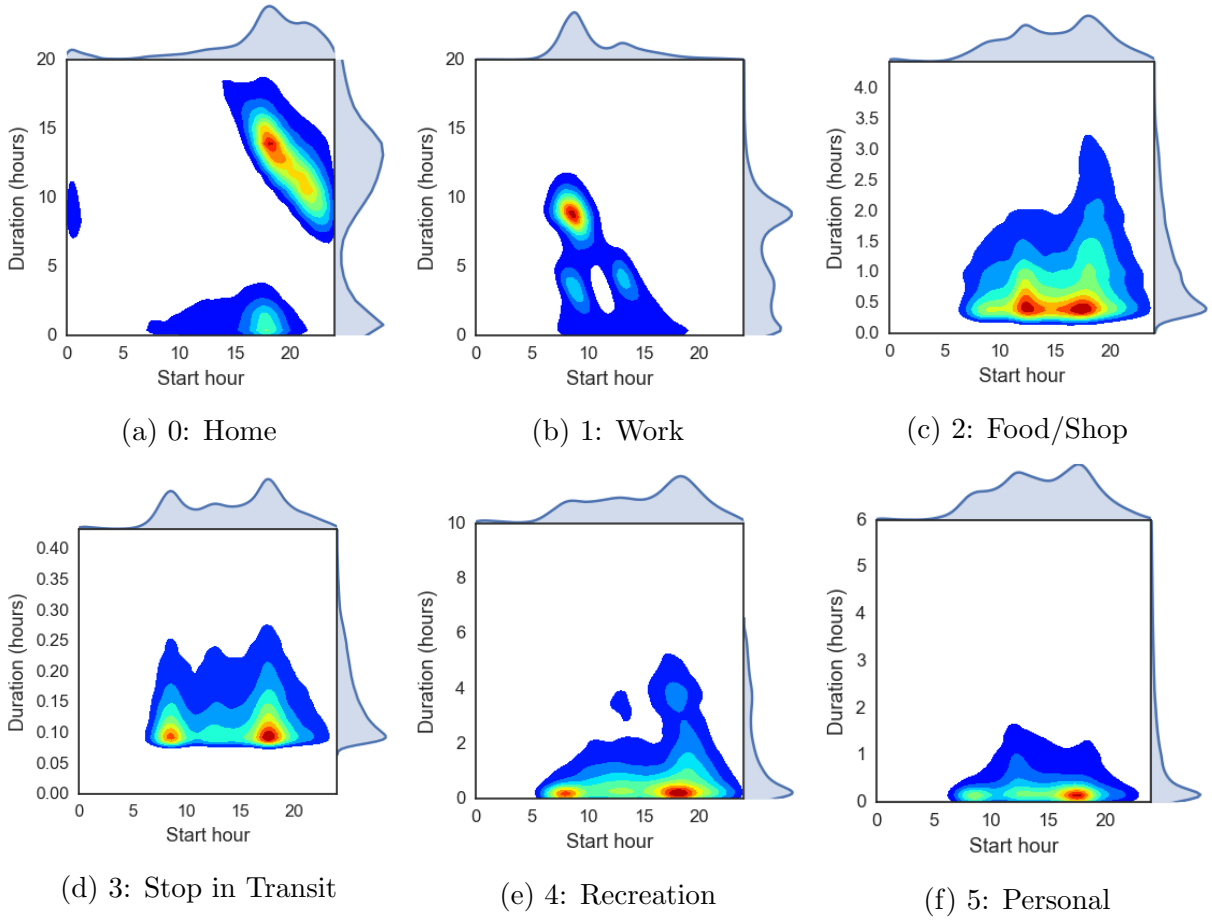

(a) 0: Home (b) 1: Work (c) 2: Food/Shop

(d) 3: Stop in Transit (e) 4: Recreation (f) 5: Personal

Figure 5.4: Joint distribution plot of duration and start hour per activity type. The labels are gained by assigning the activity to the one with the highest posterior probability after training.

transition is from "home" to "work." Fig. 5.5b shows the transition matrix associated with evenings. The transitions from all other states to "home" are significant. However, if the user's transition from activity is "home", then she is more likely to transition to "food" or "recreation" activities. Fig. 5.5c shows the transition matrix in the afternoon, for users who have not yet visited the "work" state in the day. For these users, there is a high probability of going to work. As in Fig. 5.5d, by keeping all the input context information equal as in the previous case, and only specifying that the simulated user has previously worked for 5 hours on that day, one can see that the probability of going to work is significantly reduced.

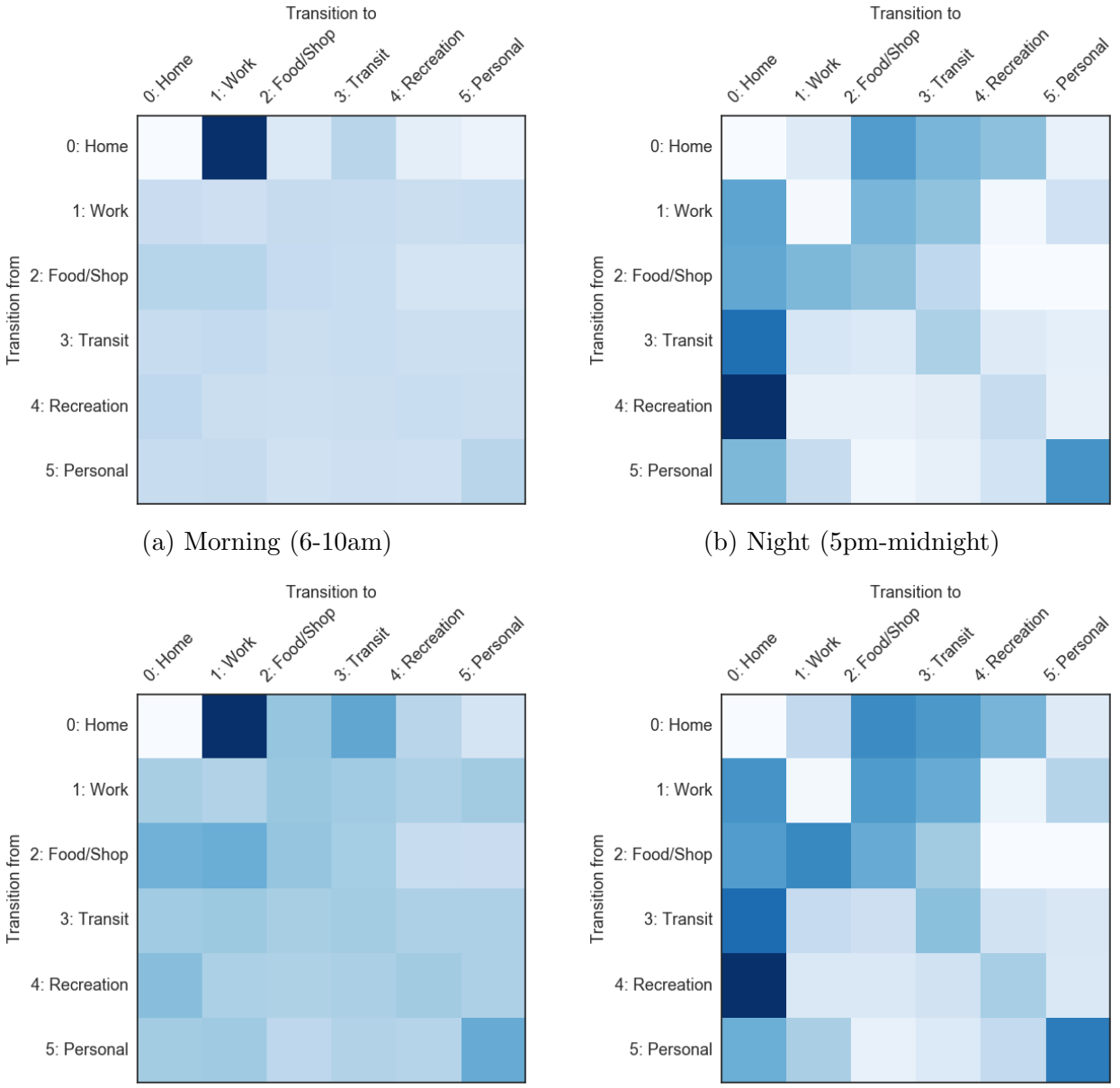

(a) Morning (6-10am)

(b) Night (5pm-midnight)

(c) Afternoon (12-2pm), users who have not visited work

(d) Afternoon (12-2pm), users who have worked 5 hours

Figure 5.5: Heterogeneous activity transition matrices under different contextual variables.

5.3 Evaluation of Activity Recognition

Recognition Accuracy

The distribution of collected ground truth activities are biased and do not correspond to the true distribution of urban activities. To reasonably evaluate performance of IO-HMM, we

Table 5.2: Confusion matrix of inferred activities versus "ground truth" activities

Ground Truth	Annotations								
	Home	Work	Food/Shop	Transit	Recreation	Personal	Travel		
Home	9994	0	0	0	1	1	4	0.999	
Work	0	7495	0	0	0	2	3	0.999	
Food/Shop	0	0	3013	413	1307	267	0	0.603	
Transit	0	0	31	6980	359	130	0	0.931	Recall
Recreation	0	0	1519	0	1403	78	0	0.468	
Personal	0	0	321	17	84	3426	152	0.857	
Travel	0	0	0	0	0	11	989	0.989	
	1.000	1.000	0.617	0.942	0.445	0.875	0.862	0.876	
	Precision								

Table 5.3: Comparison of model accuracy

Model	All Activities		Secondary Activities	
	Accuracy	F1	Accuracy	F1
HMM	0.859	0.783	0.739	0.698
Partial IO-HMM	0.866	0.824	0.752	0.754
Full IO-HMM	**0.876**	**0.827**	**0.771**	**0.758**

need to sample a subset of ground truth activities so that the sample weight is consistent with the true distribution of urban activities. According to the the distribution given by the 2015 Travel Decisions Surveys (TDS), conducted by San Francisco Municipal Transportation Agency (SFMTA)[31], we sampled (scaled) 10000 home activities, 7500 work activities, 5000 Food/Shop activities, 7500 Stop in Transit activities, 3000 recreation activities, 4000 personal activities and 1000 Travel activities.

Overall, we get 87.6% accuracy on all activities, with a macro-precision of 82%, a macro-recall of 83.5% and a macro-f1 score of 0.827. Here we reiterate that there are no explicit ground truth labels on traveler's activities; instead the ground truth labels refer to the identifiable activities that occur near short-range antennas (labeled according to Table 4.2) and activities that occur at the inferred home or work location.

From the confusion matrix in Table 5.2, we can see that most confusion happens between "food/shop" and "recreation" activities. This is natural because "food/shop" and "recreation" activities are similar in time and space. We also notice that some "food/shop" activities are mistaken as a "short stop in transit", this is because some "food/shop" activities and "stop in transit" are close in space, thus some short "food/shop" activities are taken as "stop in transit" because of the duration. Since the activities that we labeled as "personal" are mainly medium distance activities that could encompass longer-distance dining, some "food/shop" activities could also be confused as "personal".

To compare the performance of different models, we also report the accuracy of (1) Hidden Markov Models (HMM) with the same output as IO-HMM but with no inputs; (2)

Partial IO-HMM with transition probabilities dependent on inputs while all emissions are only conditioned on hidden states; and (3) Full IO-HMM as described, in Table 5.3.

We report the accuracy and macro-f1 score as metrics of success for our models. F1 score can be interpreted as a weighted average of the precision and recall. For multi-class tasks, macro-f1 score calculates the average per-class precision and recall and then perform the f1 score calculation. We can see that the full IO-HMM has the best performance. Since "home" and "work" are rather easy to infer, we also report the performance for secondary activities only. For the five class classification task, we get 77.1% accuracy. Another observation is that the macro-f1 score of the partial and full IO-HMMs do not differ too much, but all outperform the pure HMM. These results exhibit the benefits of the context-dependent transition models.

We see that the full IO-HMM outperforms the partial IO-HMM slightly which outperforms the pure HMM. Since "home" and "work" have high accuracy, the improved performance is mainly in secondary activity recognition. In all cases, f1 score is smaller than the accuracy. This is because the class that has higher support also has higher accuracy. Since accuracy score is a weighted average with support while macro-f1 score is an unweighted average, f1 score is lower than the accuracy.

Survey-derived statistics

Another way to evaluate the method is to compare our model with aggregated statistics from surveys. We consider the Travel Decisions Survey (TDS), which contains 1000 random digit dial and cell phone samplings in the area of interest. Overall, the activity proportions of our model match with TDS. If we split our Food/Shop activities into half food and half shop, food and recreation is 20% in our model versus 21% in TDS; shopping and errand (personal) is 21% in our model versus 20% in TDS. Work/school activity is 22.5% in our model versus 23% in TDS. The main difference is with the "Home" activity, for which TDS report a proportion of 35%, which is a little higher than the proportion of 30% reported by our model. This discrepancy is likely due to under-reporting of secondary activities in TDS.

5.4 Activity Generation from an IO-HMM

One of our goals is to enable activity based travel demand models that use cellular data to create synthetic agent travel patterns without compromising the privacy of cell phone users. As such, we test our models' generative power in the Bay Area context — we simulate $463,000$ agents in the Bay Area (15% sample of the commuters) and create a day-long activity plan for all agents with anticipated start-times, locations, and durations of all activities in the day.

As travel patterns vary greatly over the region, we trained 34 IO-HMMs, each for a subset of cell phone users residing within each of the 34 super-districts as defined by the San Francisco Metropolitan Transportation Commission (MTC). Using the Iterative Proportional

Fitting [14] procedure to fit the population marginals with the census data, we sample residents home and work locations to create synthetic driver with a predetermined home TAZ and work TAZ. The numbers were further adjusted according to occupancy statistics from CHTS (single driver, two and multi-person carpool). The precise home and work locations (lat/lon coordinates) are sampled uniformly within the home and work TAZs.

Each simulated user is assumed to start her day at home. The home departure time and the transition time are drawn from their respective distributions to determine the start time of the first activity. Home departure times for the first non-home activity of the day are modeled as Gaussian random variables with super-district dependent mean departure time and standard deviation calibrated from CDR records. As IO-HMM is trained on the observed travel sequences with *revealed* departures times, we assume that it captures the dependencies of transition times on the origin and destination, travel mode and traffic conditions.

Generation continues until the activity start time reaches midnight. At every step, previous activity state and context information are used to obtain transition probabilities from the IO-HMM and sample the next activity state according to the transition probabilities. After the activity type has been selected, the activity duration is sampled from a truncated normal distribution with mean and standard deviation coming from output $x^{(3)}$ of the IO-HMM. Next, the activity location is selected - if the activity is a home-activity or work-activity, the exercise is trivial. If not, we use IO-HMM outputs $x^{(1)}$ and $x^{(2)}$ - the distance between the stay location and the user's home output and distance from the stay location to the user's work output from the IO-HMM to generate a new destination TAZ from the choice set of TAZs within matching distances. The precise location of the activity is sampled uniformly from the selected TAZ. Note that future research on destination location choice models could improve the location selection process for secondary activities.

Due to the nature of IO-HMM, we must filter out and discard unrealistic activity chains generated in this process. We determine unrealistic activity chains to be chains that do not end the day at home and activity chains where 3 or more of the same activity type occur in a row. These filters constrain the overall structure of the day to be aligned with a feasible/conventional day structure. For simulation purposes we also filter activity chains that include long-distance travel out of the Bay Area. Fig. 5.6 presents 4 common and interesting (among top 20) activity patterns generated from IO-HMM model.

Overall, the aggregated statistics of activity patterns match with the travel surveys. For example, the percentage of US employed person who go to work on an average weekday is 82.9% [25], this number is 83.7% for our simulated population. Considering the summary statistics for people who go to work, we compare the percentage of people who participate in activities at different times of day. The percentage of people participating in at least one activity before morning commute, during morning commute and after work is 3.1%, 14.8% and 46.3% in the Bay Area Travel Survey [6] and these numbers are 2.9%, 15.2% and 43.7% in our simulated population.

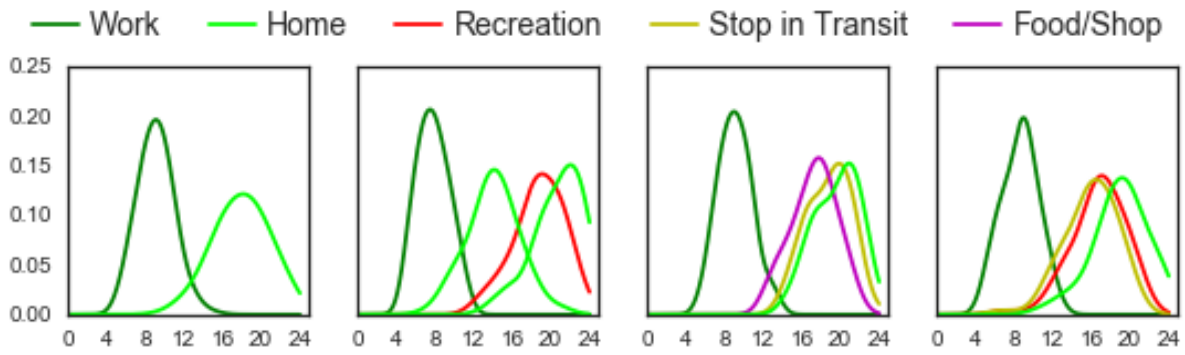

Figure 5.6: Distribution of activity start times over a course of a day of four example common activity patterns generated from the Bay Area IO-HMMs. Note that all simulated activitity patterns start at home, so (a) designates the Home-Work-Home travel pattern. The x-axis designates the start time of the activity, the y-axis represents the proportion of trips (for users with this activity pattern) starting at this time.

5.5 Evaluation via Traffic Micro-simulation

Traffic micro-simulation is a conventional approach in studying performance and evaluating transportation planning and development scenarios. Ground truth observations of the flows at sections of the road network provide an independent data source that can be used to evaluate the accuracy of the activity generation model. We present here a summary of the validation results based on the traffic volume data collected by the California DOT freeway Performance Management System (PeMS) in the 9 counties of the Bay Area (see Fig. 5.7). Micro-simulation of a typical weekday traffic is performed using the MATSim platform [2]. MATSim is a state-of-the-art agent based traffic micro-simulation tool that performs traffic assignment for the set of agents with pre-defined activity plans. It varies departure times and routing of each agent depending on the congestion generated on the network, in order to maximize agent's daily utility score. We have compared the results of the flows produced on the Bay Area network containing all freeways and primary and secondary roads (a total of 24'654 links) from the generated activity sequences with the observed traffic volumes. As the model is trained to reproduce average weekday, hourly traffic volumes are taken as averages over all weekdays (except for Mondays and Fridays) of Summer 2015. The simulation is run at 15% of the total population, and the road capacities as well as total resulting counts are scaled accordingly.

Note that observed traffic counts are not used for model calibration. They are used as independent data to evaluate the validity of the synthetic travel sequences produced with IO-HMM. The locations of the sensors on the road network are presented in Fig. 5.7. It also demonstrates examples of the three characteristic hourly volume profiles comparing the modeled and observed counts. The results for the full set of sensors are presented

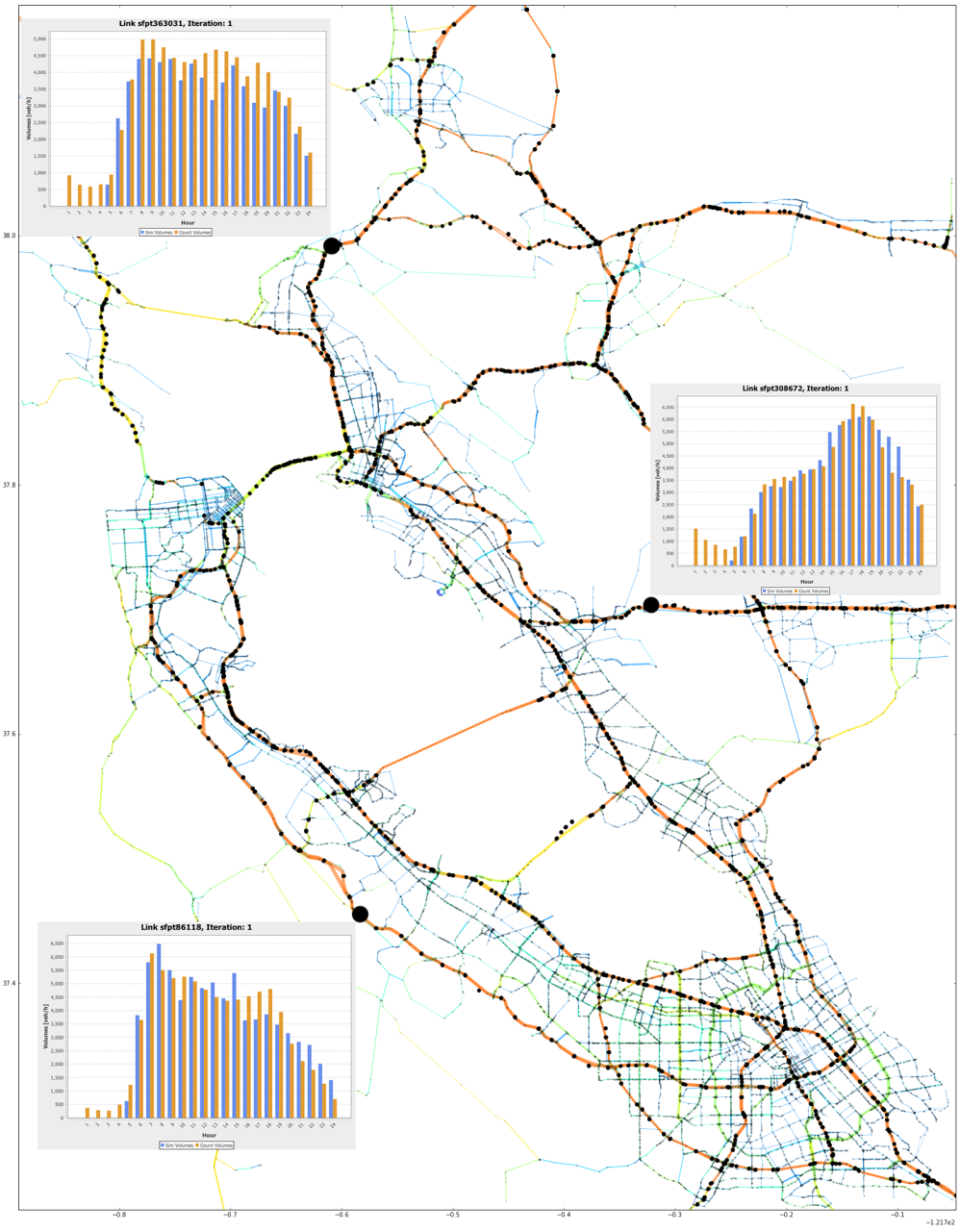

Figure 5.7: A fragment of the SF Bay Area road network with the location of 600 traffic volume detectors used for validation (shown with small black dots). Inlet graphs illustrate three sample hourly vehicle volume profiles for observed (orange) and modeled (blue) flows on a typical weekday in Summer 2015.

in Fig. 5.8. Fig. 5.8a shows a comparison of the volumes for three distinct time periods. Fig. 5.8b summarizes the validation results over all 600 sensors in terms of the relative error

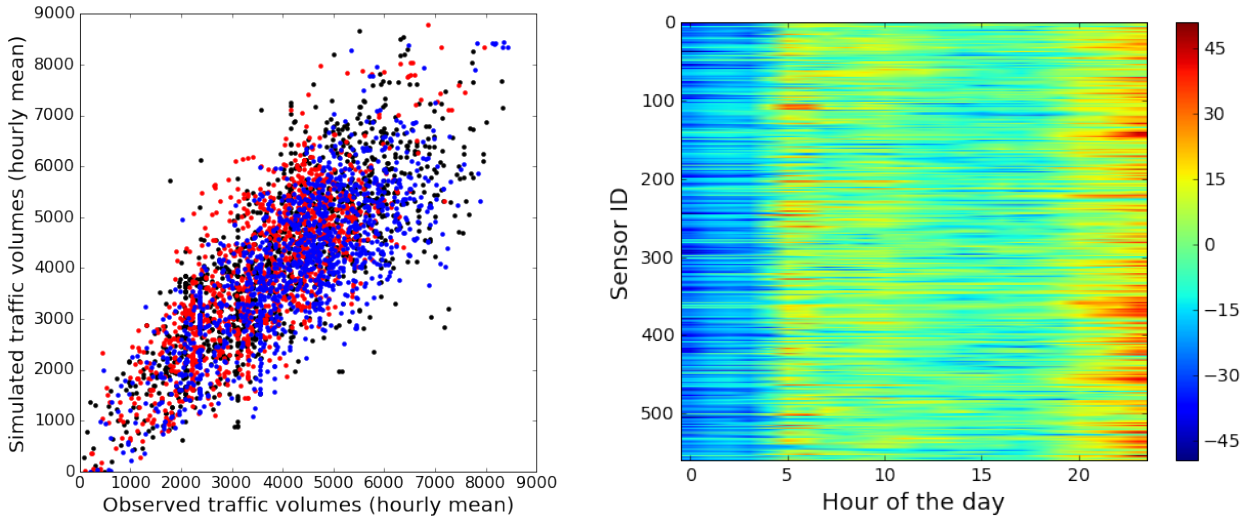

(a) Modeled versus observed volumes at 8am (black),1pm (red) and 6pm (blue) ($r^2 = 0.81, p < 10^{-3}$).

(b) Mean relative error (%) over all 600 sensors of modeled versus observed traffic volumes during the day over all 600 sensors.

Figure 5.8: Micro-simulation validation with the observed freeway traffic volumes

(% volume) over-/under-estimated by the model as compared to the ground truth. One can notice lower accuracy at night and early morning hours explained by the fact that the model was developed and applied on a subset of daily commuters and did not include a large portion of trips performed by unemployed population and people working from home, besides multiple other traffic components (commercial fleets, taxis, visitors) that are out of scope of the model. Despite it's relative simplicity, the model has demonstrated a reasonable accuracy ($r^2 = 0.81, p < 10^{-3}$ in Fig. 5.8a) as compared to the ground truth data. A thorough comparison between the activity chains generated from IO-HMM model and baseline models such as the one developed by regional transportation planning authorities and based on surveys is ongoing and its preliminary results are available from the author by request.

Chapter 6

Conclusion and Future Work

In this paper, we developed a scalable and interpretable model for regional mobility analysis from cellular data. As an illustration, we inferred the activity patterns including primary, secondary activities and heterogeneous activity transitions of a set of anonymized San Francisco Bay Area commuters using an unsupervised generative state-space model. We validated this inference by comparing it with (1) 2015 Travel Decisions Surveys (TDS) on the aggregated activity statistics; and (2) a set of ground truth activities based on short range distributed antenna system (DAS); (3) observed volumes of vehicular traffic flow in the regional road network on an average weekday. To examine the generative power of the model, we synthesized travel plans for each agent with home and work locations sampled from census data. An agent-based microscopic traffic simulation was conducted to compare the resulting traffic with real traffic, and a reasonable fit accuracy was observed. An interesting extension to this work is to compare the activity sequence generation power of different techniques, from baseline models with only home and work activities to more advanced IO-HMM models and recurrent neural network such as long short term memory (LSTM) models.

Several improvements can be built upon the presented work. Partitioning a population into sub-groups (whether socially or spatially) for shared parameter modeling is a partly open problem. Currently we approached it by defining rules to identify groups of a similar day structure, and applying geographic constraints. This step will be compared to an alternative specification that involves a mixture of IO-HMM models.

With privacy concerns and data limitations in mind, the location choice model implemented in this paper is relatively simple. Future work may incorporate a discrete choice model on a set of TAZs so that locations can be directly sampled when generating activity sequences.

Activity patterns inferred and analyzed in this paper reveal the spatial and temporal profile of activities of regular commuters, as well as the heterogeneous transition probabilities dependent on contextual information. The generative nature of our proposed model allows to sample accurate travel scenario inputs needed by activity based travel micro-simulation models. A range of issues remain where the advantages of using cellular data alone are not straightforward. This includes travel mode detection, identification of the number of

car-pools, modeling short-range and non-motorized travel to name a few. Nevertheless, such methods derived from automatically and continuously collected cell phone data are bound to make a substantial impact on urban and transportation planning, and represent a significant improvement upon the state-of-the-art.

Appendix A

Stay points detection in CDR

The goal of stay location recognition is to turn CDR logs into a list of sequential stay location identifiers with start time and duration for each user, as illustrated in Fig. 3.2. Each record of raw CDR logs contains the timestamp and the approximated latitude and longitude of events recorded by the data provider. This is a CDR-specific step that requires fine-tuning of several threshold parameters. Note that once the pre-processing steps described in this Appendix and the following are applied, only features associated with clusters locations are used, such as distances to home and work. This can be seen as a layer of anonymization of user's locations, since no specific location cluster IDs are further associated with any user at any time in the activity modeling process itself. The main steps of the algorithm are as follows:

(1) Cluster CDR records. The first step in stay location detection is filtering out positioning errors. This is achieved by spatial clustering. For GPS data, accuracy ranges of 10-100m are used in many studies that use GPS to detect stay locations [11]. The distance thresholds for GPS stay-location clustering is much smaller than the thresholds for CDR records. For example, a roaming distance of 300 meters [20] and 1000 meters [35] was used to cluster points to reflect the spatial measurement accuracy of the CDRs. For our stay-location detection, we use a density based clustering with similar parameters. At the end of the clustering step, consecutive data points with the same cluster ID are combined into a single record with start time equal to the timestamp of the first of the consecutive events at that cluster, and end time equal to the time stamp of the last of the consecutive events at that location cluster.

(2) Construct and process an oscillation graph. Consecutive CDR records may have nearly identical timestamps, but different location IDs. Such oscillations occur because the cell phone is communicating with multiple cell towers. These instantaneous location jumps may occur because of traveling users whose cell phone have just come in contact with a new cell tower along the way, but often such location jumps are observed even though users are standing still. In the latter case a user's location appears to oscillate back and forth between two clusters.

When a user's location is simultaneously reported in two location clusters, an edge be-

tween these two clusters is added to the oscillation graph. Edges in the oscillation graph connect clusters that are suspicious for oscillations.

(3) Filter oscillation points. With cluster-pairs transformed into an oscillation graph, one can discern oscillations from travel based on the pattern of location cluster sequences. Suppose the locations of two consecutive records are location cluster A and location cluster B, respectively. If edge (A, B) exists in the oscillation graph, and if the user visits cluster A, then B, back and forth, the visit to B is determined to be an oscillation - the points are combined into a single record with a duration determined by the combined time spent in A and B. We assign the location of these records to cluster A if the user spends more time in A than B, else it is assigned to cluster B.

(4) Filter locations with short durations. At this point, positioning noise and oscillation noise are removed. Now we have a sequential list of location cluster visits, each with a start and end time. Some of these cluster visits are stay locations, and others are pass-by points. The accepted threshold for stay locations varies widely. The threshold was set to 20 minutes in [37], 15 minutes in [35] and 10 minutes in [20]. Several GPS applications use stay durations ranging from 90 seconds to 10 minutes. We chose a threshold of 5 minutes, because in the activity based modeling context, 5 minutes is an appropriate threshold for an activity location, as opposed to a way-point.

Appendix B

Home and Work Inference

We recognize the importance of long-term recurrent stay points such as "home" and "work" that enforce a structure in the users' daily mobility. Various strategies have been used for home and work location detection. A mixture of Gaussians is a popular method to model locations centered on home and work [7]. Another suggested definition of "home" was the location where the user spends more than 50% of time during night hours with night hours defined as 8pm to 8am [24]. Similarly, work hours can be defined as the area where the user spends more than 50% of time during day hours.

We adopt accepted methods in order to simplify processing and, most importantly, infer "anchor" points in the daily sequences that provide space-time context that is crucial to build a generative model of secondary activities. A range of travel choices, such as mode of transportation and destination choice, depend on the overall structure of the day. Moreover, early identification of home and work allows pre-clustering users into groups with similar behaviors by using heuristic decision rules (employed/unemployed/part-time worker, etc).

Our detection of the home and work locations is similar to the method of [24]. We identify home as the location where the user spends the most stay hours during home hours, and we identify work as the location where the user spends the most hours during the work hours. However, we define home and work hours to be much narrower time windows than the 8am-8pm criteria used in [24]. Borrowing from [20], the hours from midnight to 6am are defined as home activity hours, and 1pm to 5pm on weekdays are defined as working hours because they capture the core set of working hours for both early and late workers [19].

Bibliography

[1] *2010-2012 California Household Travel Survey Final Report Appendix*. http://www.dot.ca.gov/hq/tpp/offices/omsp/statewide_travel_analysis/files/CHTS_Final_Report_June_2013.pdf.

[2] M Balmer et al. *Agent-based simulation of travel demand: Structure and computational performance of MATSim-T*. ETH, Eidgenössische Technische Hochschule Zürich, IVT Institut für Verkehrsplanung und Transportsysteme, 2008.

[3] Mitra Baratchi et al. "A hierarchical hidden semi-Markov model for modeling mobility data". In: *Proceedings of the 2014 ACM International Joint Conference on Pervasive and Ubiquitous Computing*. ACM. 2014, pp. 401–412.

[4] Moshe Ben-Akiva and Bruno Boccara. "Discrete choice models with latent choice sets". In: *International Journal of Research in Marketing* 12.1 (1995), pp. 9–24.

[5] Yoshua Bengio and Paolo Frasconi. "An input output HMM architecture". In: (1995).

[6] Chandra R Bhat and Sujit K Singh. "A comprehensive daily activity-travel generation model system for workers". In: *Transportation Research Part A: Policy and Practice* 34.1 (2000), pp. 1–22.

[7] Eunjoon Cho, Seth A Myers, and Jure Leskovec. "Friendship and mobility: user movement in location-based social networks". In: *Proceedings of the 17th ACM SIGKDD international conference on Knowledge discovery and data mining*. ACM. 2011, pp. 1082–1090.

[8] Pierre Deville et al. "Dynamic population mapping using mobile phone data". In: *Proceedings of the National Academy of Sciences* 111.45 (2014), pp. 15888–15893.

[9] Nathan Eagle and Alex Sandy Pentland. "Eigenbehaviors: Identifying structure in routine". In: *Behavioral Ecology and Sociobiology* 63.7 (2009), pp. 1057–1066.

[10] Vincent Etter et al. "Where to go from here? Mobility prediction from instantaneous information". In: *Pervasive and Mobile Computing* 9.6 (2013), pp. 784–797.

[11] Yingling Fan et al. "SmarTrAC: A smartphone solution for context-aware travel and activity capturing". In: (2015).

[12] Katayoun Farrahi and Daniel Gatica-Perez. "A probabilistic approach to mining mobile phone data sequences". In: *Personal and ubiquitous computing* 18.1 (2014), pp. 223–238.

[13] Katayoun Farrahi and Daniel Gatica-Perez. "Discovering routines from large-scale human locations using probabilistic topic models". In: *ACM Transactions on Intelligent Systems and Technology (TIST)* 2.1 (2011), p. 3.

[14] Stephen E. Fienberg. "An Iterative Procedure for Estimation in Contingency Tables". In: *The Annals of Mathematical Statistics* 41.3 (1970), pp. 907–917. ISSN: 00034851. DOI: 10.2307/2239244. URL: http://dx.doi.org/10.2307/2239244.

[15] João Bártolo Gomes, Clifton Phua, and Shonali Krishnaswamy. "Where will you go? mobile data mining for next place prediction". In: *Data Warehousing and Knowledge Discovery*. Springer, 2013, pp. 146–158.

[16] Marta C Gonzalez, Cesar A Hidalgo, and Albert-Laszlo Barabasi. "Understanding individual human mobility patterns". In: *Nature* 453.7196 (2008), pp. 779–782.

[17] Ramaswamy Hariharan and Kentaro Toyama. "Project Lachesis: parsing and modeling location histories". In: *Geographic Information Science*. Springer, 2004, pp. 106–124.

[18] David T Hartgen and Elizabeth San Jose. *Costs and Trip Rates of Recent Household Travel Surveys*. 2009.

[19] Sibren Isaacman et al. "Identifying important places in peoplefffdfffdfffds lives from cellular network data". In: *Pervasive computing*. Springer, 2011, pp. 133–151.

[20] Shan Jiang et al. "A review of urban computing for mobile phone traces: current methods, challenges and opportunities". In: *Proceedings of the 2nd ACM SIGKDD International Workshop on Urban Computing*. ACM. 2013, p. 2.

[21] *Jobs per Square Mile*. http://http://www.sustainablecommunitiesindex.org/indicators/view/209.

[22] Youngsung Kim et al. "Activity recognition for a smartphone based travel survey based on cross-user history data". In: *2014 22nd International Conference on Pattern Recognition (ICPR)*. IEEE. 2014, pp. 432–437.

[23] Felix Kling and Alexei Pozdnoukhov. "When a city tells a story: urban topic analysis". In: *Proceedings of the 20th international conference on advances in geographic information systems*. ACM. 2012, pp. 482–485.

[24] Kevin S Kung et al. "Exploring universal patterns in human home-work commuting from mobile phone data". In: (2014).

[25] US Bureau of Labor Statistics. *AMERICAN TIME USE SURVEY fffdfffdfffd 2015 RESULTS*. Tech. rep. June 2016.

[26] Lin Liao, Dieter Fox, and Henry Kautz. "Extracting places and activities from gps traces using hierarchical conditional random fields". In: *The International Journal of Robotics Research* 26.1 (2007), pp. 119–134.

[27] Lin Liao, Dieter Fox, and Henry Kautz. "Hierarchical conditional random fields for GPS-based activity recognition". In: *Robotics Research*. Springer, 2007, pp. 487–506.

[28] Feng Liu et al. "Annotating mobile phone location data with activity purposes using machine learning algorithms". In: *Expert Systems with Applications* 40.8 (2013), pp. 3299–3311.

[29] Xin Lu, Linus Bengtsson, and Petter Holme. "Predictability of population displacement after the 2010 Haiti earthquake". In: *Proceedings of the National Academy of Sciences* 109.29 (2012), pp. 11576–11581.

[30] Santi Phithakkitnukoon et al. "Activity-aware map: Identifying human daily activity pattern using mobile phone data". In: *Human Behavior Understanding*. Springer, 2010, pp. 14–25.

[31] San Francisco Municipal Transportation Agency (SFMTA). *Travel Decisions Survey 2015*. Tech. rep. 2015.

[32] Adella Santos et al. *Summary of travel trends: 2009 national household travel survey*. Tech. rep. 2011.

[33] Chaoming Song et al. "Limits of predictability in human mobility". In: *Science* 327.5968 (2010), pp. 1018–1021.

[34] Pu Wang et al. "Understanding road usage patterns in urban areas". In: *Scientific reports* 2 (2012).

[35] Peter Widhalm et al. "Discovering urban activity patterns in cell phone data". In: *Transportation* 42.4 (2015), pp. 597–623.

[36] Jihang Ye, Zhe Zhu, and Hong Cheng. "What's your next move: User activity prediction in location-based social networks". In: *Proceedings of the SIAM International Conference on Data Mining. SIAM*. 2013.

[37] Yu Zheng et al. "Mining interesting locations and travel sequences from GPS trajectories". In: *Proceedings of the 18th international conference on World wide web*. ACM. 2009, pp. 791–800.

[38] Yu Zheng et al. "Urban computing: concepts, methodologies, and applications". In: *ACM Transactions on Intelligent Systems and Technology (TIST)* 5.3 (2014), p. 38.